Eleventh International Conference on Computational Fluid Dynamics (ICCFD11), Maui, Hawaii, July 11-15, 2022

ICCFD11-2022-2401

Fully-automated high-fidelity LES around high-lift aircraft configuration near stall

H. Asada* and S. Kawai*
Corresponding author: h.asada@tohoku.ac.jp

* Department of Aerospace Engineering, Tohoku University, Japan.

Abstract: This study presents the large-eddy simulation (LES) around a high-lift aircraft configuration at near-stall conditions. In the present LES, we employ the non-body-fitted hierarchical Cartesian grid and achieve fully automated grid generation for the complex aircraft configuration. The wall modeling is also adopted to realize the LES of high-Reynolds-number flows, and this study performs the wall-modeled LES around the complex aircraft configuration by utilizing the wall modeling on non-body-fitted Cartesian grids. Furthermore, we use the kinetic-energy and entropy preserving (KEEP) scheme, which is stable and non-dissipative, to achieve stable high-fidelity simulations. The number of grid points is over 10 billion, and the state-of-the-art supercomputer Fugaku is used for massively parallel computations. The present wall-modeled LES successfully predicts the complex flowfield involving separation around the high-lift aircraft configuration and aerodynamic forces at the near-stall conditions, without numerical instability.

Keywords: Large-eddy simulation, high-lift aircraft, hierarchical Cartesian grid, wall modeling.

1 Introduction

The predictions of aerodynamic forces exerted on aircraft at near-stall conditions (i.e., maximum lift) are challenging. Actually, in the CFD High Lift Prediction Workshop (HiLiftPW) [1, 2, 3, 4], various CFD solvers gave the significant variation of the predicted lift coefficients for a full aircraft configuration near stall. One of the reasons for the variations of the predicted lift coefficients may be the dependency of turbulence models used in Reynolds-averaged Navier–Stokes (RANS) simulations, which becomes notable particularly for the complex turbulence such as separated flows. On the other hand, large-eddy simulation (LES) is suitable for simulating complex turbulence because the model dependency of LES is much lower than the RANS simulations. Prior studies performed the LES for elucidating the physics of complex turbulence in, for example, transitional flows [5], separated flows [6], transonic airfoil buffet [7], heated/cooled high-speed flows [8], etc.

However, the LES around a full aircraft configuration for predicting the maximum lift is also challenging. This is because small complex devices substantially affects the aerodynamic forces near stall, and thus numerical simulations need to handle the complex geometries to predict the aerodynamic forces accurately. The prior LES employed structured grids around relatively simple geometries, which are not suitable for the complex geometries. The popular methods for handling the complex geometries are unstructured grids. Nevertheless, the generation of the unstructured grids requires time-consuming human efforts for very complex geometries such as a landing gear [9]. Furthermore, the high-Reynolds-number flows at the real-flight conditions also make the LES around the full aircraft configuration difficult. The Reynolds number effects on the aerodynamic forces near stall are notable, and thus LES of high-Reynolds-number flows are necessary. However, the LES of high-Reynolds-number flows requires prohibitively high mesh density near walls to resolve thin boundary layers. Indeed, Choi and Moin [10] estimated the required number of grid points in the LES as $N \propto Re_c^{13/7}$, which becomes quite high for Reynolds number of $Re_c \approx 10^7$ at the real-flight condition.

This study overcomes the problems described above and realizes the LES of high-Reynolds-number flows around the full aircraft configuration for predicting aerodynamic forces near stall. We employ the non-body-fitted hierarchical Cartesian grid [9, 11] to handle the complex aircraft configuration and achieve fully automated grid-generation for complex aircraft configuration, with only the input of geometrical data. Also, the wall modeling [12, 13, 14] for inner-layer turbulence is utilized to dramatically reduce the required number of grid points in the LES of high-Reynolds-number flows, and this study exploits the wall modeling on non-body-conforming boundaries [15] to realize the wall-modeled LES on the hierarchical Cartesian grids. Furthermore, we adopt the kinetic-energy and entropy preserving (KEEP) scheme [16, 17, 18], which is a non-dissipative and stable scheme for convective terms, to achieve high-fidelity simulations. This study implements these three key numerical methods in the compressible flow solver FFVHC-ACE and apply FFVHC-ACE to the wall-modeled LES around the full aircraft configuration. The simulated full aircraft configuration is the JAXA standard model (JSM) [19], and we perform the predictions of complex flows and aerodynamic forces at the near-stall conditions. The large-scale simulations are conducted with the grid points over 10 billion, and the state-of-the-art supercomputer Fugaku is used for massively parallel computations. The obtained results are compared to the experimental data reported in the 3rd HiLiftPW [4].

2 Numerical methods

2.1 Hierarchical Cartesian grids

The hierarchical Cartesian grid [9, 11]is a block-based non-body-fitted Cartesian grid, which is a recently reconsidered method for treating complex geometries. In the hierarchical Cartesian grid, the computational domain is simply divided by cubes called computational blocks, and the equally spaced Cartesian grids are generated by dividing each block. The local grid refinements for small flow scales such as boundary layers and wakes are achieved by giving additional blocks at the regions of the small flow scales. This study employs the octree data structure for generating the computational blocks. The simple algorithms of grid-generation provide the fast and effective grid generation, and this study achieves the fully automated grid generation for the complex aircraft configuration only with the input of STL data, even when the number of grid points becomes over 10 billion. Although the wall boundaries are step-like on the non-body-fitted hierarchical Cartesian grid, this study employs the wall boundary conditions given by the wall modeling on non-body-conforming block boundaries [15], as discussed in the next section.

2.2 Wall modeling on non-body-conforming boundaries

Tamaki and Kawai [15] propose the wall modeling on non-body-conforming boundaries to realize the LES of high-Reynolds-number flows on the non-body-fitted Cartesian grids. Their wall modeling predicts the wall shear stress in the turbulent boundary layers through the wall functions, which is solved with the wall-parallel velocities at the image points (IPs) installed in the wall-normal direction. The predicted wall shear stress is used as the boundary conditions in the LES. Although the conservation errors near the non-body-conforming boundaries violate the total shear stress balance and deteriorate the prediction accuracy of the wall shear stress, Tamaki and Kawai [15] propose to employ the partial-slip condition instead of the non-slip condition as

$$U_w = U_{\mathrm{IP}} - \left.\frac{dU}{dY}\right|_{\mathrm{IP}} Y_{\mathrm{IP}}, \tag{1}$$

where U_w is the velocity at the wall, U_{IP} is the velocity at the IPs, and Y is the distance from the wall. The use of the partial-slip condition reduces the velocity gradient and thus improves the resolution for the velocity gradient, which reduces the conservation errors and enhances the prediction accuracy of wall shear stress. Furthermore, to remedy the reduced shear stress caused by the partial-velocity gradient, Tamaki and

Kawai [15] proposes the modeled turbulent shear stress $\tau_{ij}^{\mathrm{model}}$ as

$$\tau_{ij}^{\mathrm{model}} = \tau_w \left(n_i t_j + t_i n_j \right) f_s, \qquad f_s = \max\left(\frac{Y - Y_{\mathrm{IP}}}{Y_{\mathrm{IP}}}, 0 \right), \tag{2}$$

where τ_w is the wall shear stress predicted by the wall functions, n_i is the unit wall-normal vector, and t_i is the unit wall-parallel vector. The modeled shear stress given by Eq. (2) is added to the viscous stress τ_{ij} calculated by the velocity gradients and sub-grid-scale models. This study sets the distance between the IPs and the walls as $Y_{\mathrm{IP}} = 3.5\Delta x_w$ according to Ref. [15], where Δx_w is the grid spacing at the walls.

2.3 Kinetic-energy and entropy preserving (KEEP) scheme

The KEEP scheme [16, 17, 18] achieves remarkable numerical stability with non-dissipative nature. The superior numerical stability is achieved by preserving the kinetic energy and the entropy at the discrete level. The KEEP scheme solves the mass, momentum, and total-energy equations as conventional compressible flow simulations, and the numerical fluxes at the cell interfaces are evaluated as

$$\begin{cases} \dfrac{\partial \rho u_j}{\partial x_j} \simeq \dfrac{C_j|_{m+1/2} - C_j|_{m-1/2}}{\Delta x_j}, \\ \dfrac{\partial \rho u_i u_j}{\partial x_j} \simeq \dfrac{M_{ij}|_{m+1/2} - M_{ij}|_{m-1/2}}{\Delta x_j}, \\ \dfrac{\partial \rho k u_j}{\partial x_j} \simeq \dfrac{K_j|_{m+1/2} - K_j|_{m-1/2}}{\Delta x_j}, \\ \dfrac{\partial \rho e u_j}{\partial x_j} \simeq \dfrac{I_j|_{m+1/2} - I_j|_{m-1/2}}{\Delta x_j}, \\ \dfrac{\partial p \delta_{ij}}{\partial x_j} \simeq \dfrac{\Pi_{ij}|_{m+1/2} - \Pi_{ij}|_{m-1/2}}{\Delta x_j}, \\ \dfrac{\partial p u_j}{\partial x_j} \simeq \dfrac{P_j|_{m+1/2} - P_j|_{m-1/2}}{\Delta x_j}, \end{cases} \quad \text{where} \quad \begin{cases} C_j|_{m\pm1/2} = \dfrac{\rho|_m + \rho|_{m\pm1}}{2} \dfrac{u_j|_m + u_j|_{m\pm1}}{2} \\ M_{ij}|_{m\pm1/2} = C_j|_{m\pm1/2} \dfrac{u_i|_m + u_i|_{m\pm1}}{2}, \\ K_j|_{m\pm1/2} = C_j|_{m\pm1/2} \dfrac{u_k|_m u_k|_{m\pm1}}{2}, \\ I_j|_{m\pm1/2} = C_j|_{m\pm1/2} \dfrac{e|_m + e|_{m\pm1}}{2}, \\ \Pi_{ij}|_{m\pm1/2} = \dfrac{p|_m + p|_{m\pm1}}{2} \delta_{ij}, \\ P_j|_{m\pm1/2} = \dfrac{u_j|_m p|_{m\pm1} + u_j|_{m\pm1} p|_m}{2}, \end{cases} \tag{3}$$

where C, M, Π, K, I, and P are numerical fluxes of the mass, momentum, pressure gradient, kinetic energy, internal energy, and pressure diffusion, respectively, and the subscript m denotes the cell index, ρ is the density, u_i is the velocity, e is the internal energy, p is the pressure, and δ_{ij} is the Kronecker delta. Note that the above numerical fluxes are split forms of the second-order central difference scheme and thus non-dissipative. These numerical fluxes preserve the kinetic energy and entropy well, which allows the remarkable numerical stability as discussed in Ref. [16]. The KEEP scheme is extended to the generalized curvilinear grid [18] and the hierarchical Cartesian grid [17] to treat the complex geometries. The KEEP scheme for the hierarchical Cartesian grids achieves the kinetic-energy and entropy preservation at the non-conforming block boundaries with hanging nodes, by appropriately assigning the variables at the ghost cells. See Ref. [17] for the detailed strategy of the KEEP scheme on the hierarchical Cartesian grid. Also, to remove the numerical oscillations generated by the KEEP scheme on the hierarchical Cartesian grids, this study employs the conservative low-pass filter for the hierarchical Cartesian grid proposed by Asada and Kawai [20]. Their conservative low-pass filter is the flux-based fourth-order explicit filter, and the conservations of the conservative variables at the non-conforming block boundaries are strictly maintained by properly evaluating the numerical flux of the filter. Although the explicit filter dumps the resolved solutions at the low-wavenumber regime, the transfer function of the explicit filter is controlled to enhance the low-pass characteristic.

3 Computational setup

This study presents the wall-modeled LES of high-Reynolds-number flows around the JAXA standard model (JSM) [19]. The JSM configuration equips the wing, fuselage, engine nacelles, and high-lift devices (i.e., slat,

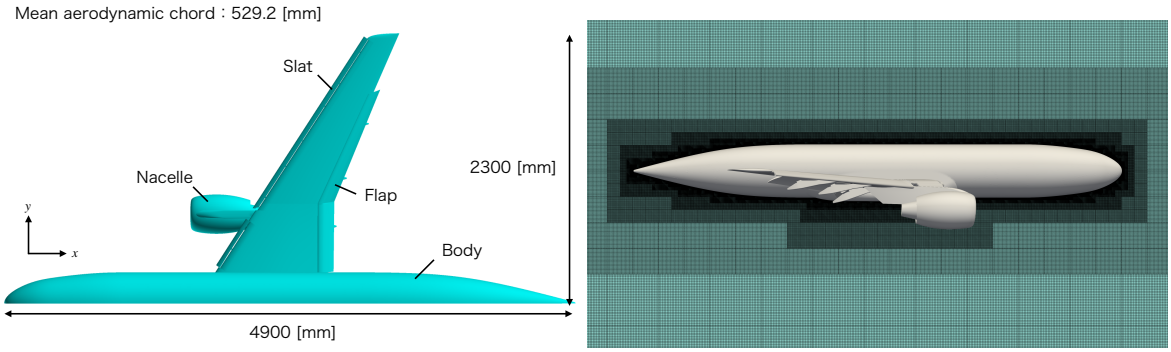

(a) Configuration (b) Hierarchical Cartesian grid

Figure 1: Configuration and hierarchical Cartesian grid for JSM.

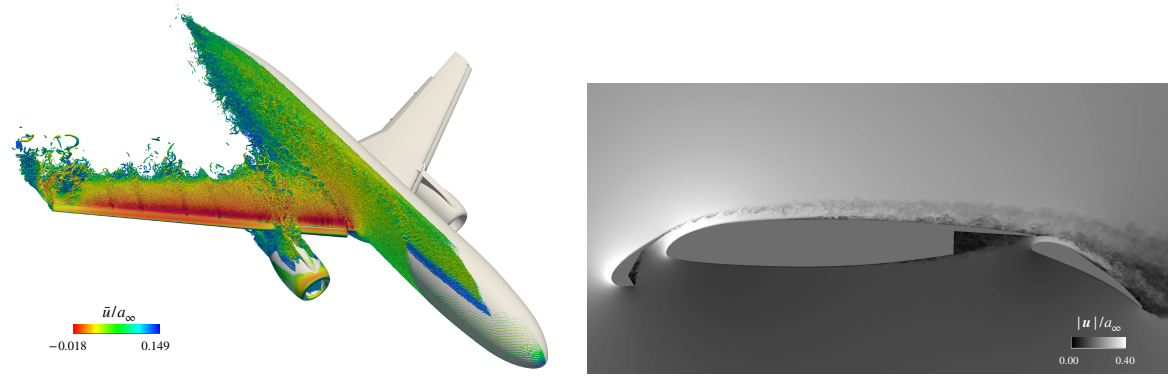

(a) Q criterion (b) Velocity magnitude

Figure 2: Iso-surface of Q criterion colored by streamwise velocity and velocity magnitude at spanwise cross-section for $\alpha = 18.58\,\mathrm{deg}$.

flap, and their supports). The computational domain is $62c_{\mathrm{MAC}}$, where c_{MAC} is the mean aerodynamic chord, and the two hierarchical Cartesian grids, Grid1 and Grid2, are generated for the half model of the JSM configuration as shown in Fig. 1. The total numbers of computational cells for Grid1 and Grid2 are 2.3 billion and 11.7 billion, respectively, and the grid spacings near the walls are $\Delta x/c_{\mathrm{MAC}} = 9.45 \times 10^{-4}$ and 4.72×10^{-4}, respectively. The supercomputer Fugaku is used for massively parallel computations. The freestream Mach number is 0.172, the chord-based Reynolds number is 1.93 million, and three angles of attack $\alpha = 10.48$, 18.58, and 21.57 deg are examined. The time integration is performed by the Euler implicit method firstly, and, after the lift coefficients are converged, the implicit method is changed to the 3step TVD Runge-Kutta explicit method. The statistics are collected during $tu_\infty/c_{\mathrm{MAC}} > 5$, and the obtained statistical data are compared to the experimental data given by the 3rd HiLiftPW [4]. In this paper, the results obtained by the wall-modeled LES with Grid2 and the KEEP scheme are shown. Further discussions, which include the grid-convergence study and the comparison between the KEEP scheme and the conventional upwind scheme, will be given in the future presentation.

4 Results & discussions

This study successfully realizes the high-fidelity LES of high-Reynolds-number flows around the complex high-lift aircraft configuration without numerical instabilities, in addition to the fully automated grid-generation.

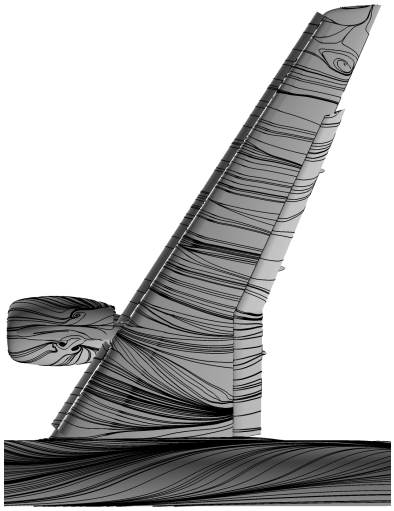

(a) Wall-modeled LES ($\alpha = 18.58\,\mathrm{deg}$)

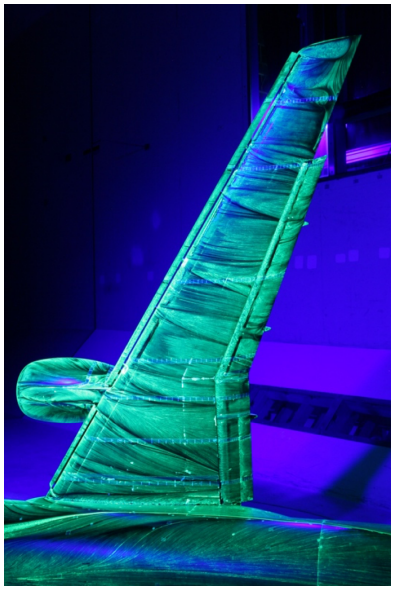

(b) Experiment ($\alpha = 18.58\,\mathrm{deg}$) [4]

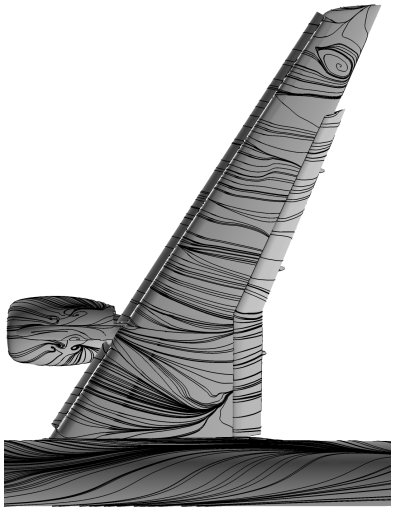

(c) Wall-modeled LES ($\alpha = 21.57\,\mathrm{deg}$)

(d) Experiment ($\alpha = 21.57\,\mathrm{deg}$) [4]

Figure 3: Streamline around JSM configuration at $\alpha = 18.58\,\mathrm{deg}$ and $21.57\,\mathrm{deg}$.

Figure 2(a) shows the instantaneous iso-surfaces of the Q criterion colored by the streamwise velocity. As well as the vortex structured of near-wall turbulence, the present wall-modeled LES simulates the longitudinal vortices generated from the slat supports, which means that the small complex geometries are treated in the LES. Figure 2(b) shows the instantaneous velocity magnitude at the spanwise cross-section. We can observe that the slat wake interacts with the boundary layers developed over the main wing, and this interaction gives the laminar-to-turbulence transition.

Figure 3 shows the time-averaged streamline to visualize the surface flow. The results of the experimental oil flow reported in the 3rd HiLiftPW [4] are also shown for comparison. The present wall-modeled LES gives good agreements of the surface flow with the experiments for both $\alpha = 18.58\,\mathrm{deg}$ and $21.57\,\mathrm{deg}$. At $\alpha = 18.58\,\mathrm{deg}$, the separated flows are formed at the outboard side. Note that the various RANS

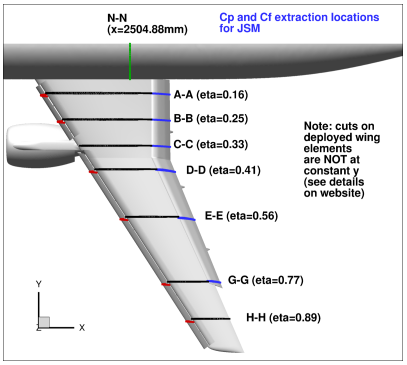

(a) Section locations [4]

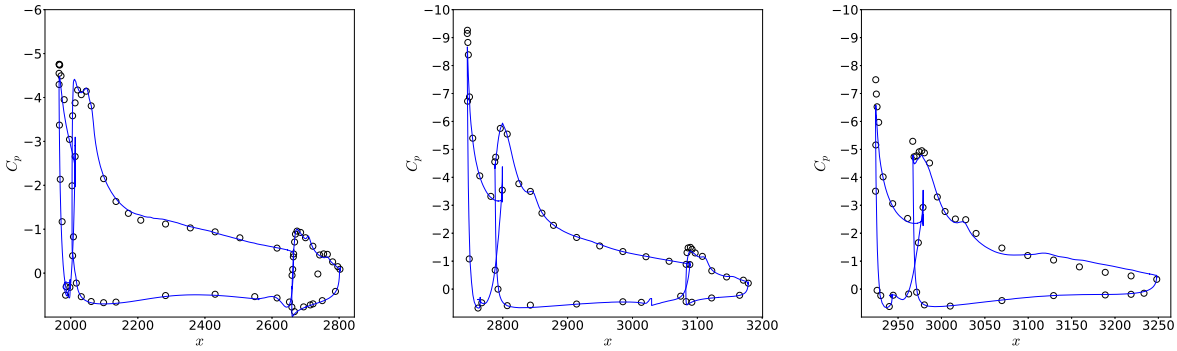

(b) Section B ($\alpha = 18.58\,\text{deg}$) (c) Section G ($\alpha = 18.58\,\text{deg}$) (d) Section H ($\alpha = 18.58\,\text{deg}$)

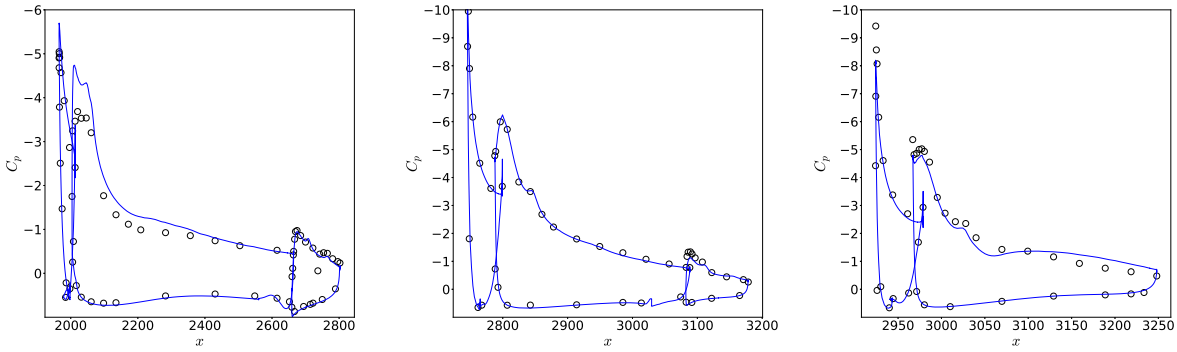

(e) Section B ($\alpha = 21.57\,\text{deg}$) (f) Section G ($\alpha = 21.57\,\text{deg}$) (g) Section H ($\alpha = 21.57\,\text{deg}$)

Figure 4: Pressure coefficient around JSM configuration at several spanwise cross-sections. —, wall-modeled LES; ○, experiment [4].

simulations shown in the 3rd HiLiftPW overpredicted the outboard separation at $\alpha = 18.58\,\text{deg}$ compared to the experiments, whereas the present wall-modeled LES predicts the outboard separation similar to the experiments. We also note that, although not shown here, Grid1 also gives good agreements with the experiments on the wall-modeled LES, which means that the grid convergence is achieved even for Grid1 at $\alpha = 18.58\,\text{deg}$. At $\alpha = 21.57\,\text{deg}$, the inboard separation emerges near the trailing edge, in addition to the outboard separation. The inboard separation near the trailing edge is also similar to the experiments. Although the inboard separation near the leading edge is not predicted in the wall-modeled LES unlike in

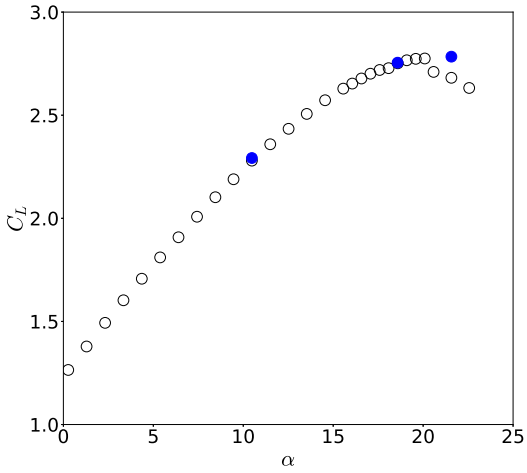

Figure 5: Lift coefficient of JSM configuration. •, wall-modeled LES; ○, experiment [4].

the experiments, we emphasize that this inboard separation near the leading edge is reported to depend the wind-tunnel-walls substantially [21]. Figure 4 shows the time-averaged pressure coefficient at several spanwise cross-sections. Good agreements of pressure distributions with the experiments are achieved by the present wall-modeled LES, particularly at $\alpha = 18.58\,\mathrm{deg}$. The high suction peaks at the inboard side (Section A) predicted by the wall-modeled LES at $\alpha = 21.57\,\mathrm{deg}$ are due to the attached inboard flow near the leading edge, as discussed in Fig. 3.

Figure 5 shows the lift coefficient obtained by the wall-modeled LES along with the experimental data. The wall-modeled LES gives reasonable agreements with the experiments for the three angles of attack. The lift coefficient at $\alpha = 21.57\,\mathrm{deg}$ predicted by the wall-modeled LES is higher than the experiments, which is again due to the attached inboard flow near the leading edge. As mentioned before, the inboard flow is substantially affected by the wind-tunnel-wall. This study will perform the large-scale simulations with further fine grid (i.e., Grid3) in the future works to clarify whether the inboard flow near the leading edge is attached or separated.

5 Conclusions

This study presents wall-modeled large-eddy simulation (LES) around a high-lift aircraft configuration at near-stall conditions. We employ the hierarchical Cartesian grid to handle the complex aircraft configuration and the wall-modeling on the non-body-fitted Cartesian grids to realize the LES of high-Reynolds-number flows around the complex aircraft configuration. Furthermore, the kinetic-energy and entropy preserving (KEEP) scheme provides stable and high-fidelity simulations because of its non-dissipative nature. Thanks to the simple grid-generation algorithms, this study achieves the fully automated grid generation around the complex aircraft configuration, and the high-fidelity LES of high-Reynolds-number flows are realized without numerical instabilities. The computed flowfield around the high-lift aircraft configuration agrees well with the experimental data, and the present wall-modeled LES predicts the aerodynamic forces at the near-stall conditions accurately.

Acknowledgments

This work was supported in part by MEXT as“ Program for Promoting Researches on the Supercomputer Fugaku ”(Leading research on innovative aircraft design technologies to replace flight test, JPMXP1020200312)

and used computational resources of supercomputer Fugaku provided by RIKEN Center for Computational Science (Project ID: hp200137, hp210168, hp220160).

References

[1] C. L. Rumsey, J. P. Slotnick, M. Long, R. A. Stuever, and T. R. Wayman. Summary of the first AIAA CFD high-lift prediction workshop. *Journal of Aircraft*, 48(6):2068–2079, 2011.

[2] C. L. Rumsey and J. P. Slotnick. Overview and summary of the second AIAA high-lift prediction workshop. *Journal of Aircraft*, 52(4):1006–1025, 2015.

[3] C. L. Rumsey, J. P. Slotnick, and A. J. Sclafani. Overview and summary of the third AIAA high lift prediction workshop. *Journal of Aircraft*, 56(2):621–644, 2019.

[4] 3rd AIAA CFD High Lift Prediction Workshop. `https://hiliftpw.larc.nasa.gov/index-workshop3.html`, accessed in 2019.

[5] S. Kawai and K. Fujii. Compact scheme with filtering for large-eddy simulation of transitional boundary layer. *AIAA Journal*, 46(3):690–700, 2008.

[6] K. Asada and S. Kawai. Large-eddy simulation of airfoil flow near stall condition at Reynolds number 2.1×10^6. *Physics of Fluids*, 30(8):085103, 2018.

[7] Y. Fukushima and S. Kawai. Wall-modeled large-eddy simulation of transonic airfoil buffet at high Reynolds number. *AIAA Journal*, 56(6):2372–2388, 2018.

[8] R. Hirai, R. Pecnik, and S. Kawai. Effects of the semi-local Reynolds number in scaling turbulent statistics for wall heated/cooled supersonic turbulent boundary layers. *Physical Review Fluids*, 6(12):124603, 2021.

[9] K. Nakahashi. Aeronautical CFD in the age of Petaflops-scale computing: From unstructured to Cartesian meshes. *European Journal of Mechanics-B/Fluids*, 40:75–86, 2013.

[10] H. Choi and P. Moin. Grid-point requirements for large eddy simulation: Chapman 's estimates revisited. *Physics of Fluids*, 24(1):011702, 2012.

[11] A. Lintermann, S. Schlimpert, J. H. Grimmen, C. Günther, M. Meinke, and W. Schröder. Massively parallel grid generation on HPC systems. *Computer Methods in Applied Mechanics and Engineering*, 277:131–153, 2014.

[12] S. Kawai and J. Larsson. Wall-modeling in large eddy simulation: Length scales, grid resolution, and accuracy. *Physics of Fluids*, 24(1):015105, 2012.

[13] J. Larsson, S. Kawai, J. Bodart, and I. Bermejo-Moreno. Large eddy simulation with modeled wall-stress: recent progress and future directions. *Mechanical Engineering Reviews*, 3(1):15–00418, 2016.

[14] S. T. Bose and G. I. Park. Wall-modeled large-eddy simulation for complex turbulent flows. *Annual review of fluid mechanics*, 50:535–561, 2018.

[15] Y. Tamaki and S. Kawai. Wall-modeling for large-eddy simulation on non-body-conforming cartesian grids. *Physical Review of Fluids*, 6(11):114603, 2021.

[16] Y. Kuya, K. Totani, and S. Kawai. Kinetic energy and entropy preserving schemes for compressible flows by split convective forms. *Journal of Computational Physics*, 375:823–853, 2018.

[17] Y. Kuya and S. Kawai. A stable and non-dissipative kinetic energy and entropy preserving (KEEP) scheme for non-conforming block boundaries on Cartesian grids. *Computers & Fluids*, 200:104427, 2020.

[18] Y. Kuya and S. Kawai. High-order accurate kinetic-energy and entropy preserving (KEEP) schemes on curvilinear grids. *Journal of Computational Physics*, 442:110482, 2021.

[19] Y. Yokokawa, M. Murayama, H. Uchida, K. Tanaka, T. Ito, and K. Yamamoto. Aerodynamic influence of a half-span model installation for high-lift configuration experiment. In *48th AIAA Aerospace Sciences Meeting Including the New Horizons Forum and Aerospace Exposition*, page 684, 2010.

[20] H. Asada and S. Kawai. Conservative low-pass filter with compact stencils for hierarchical Cartesian mesh. 2021. submitted.

[21] Y. Ito, M. Murayama, Y. Yokokawa, K. Yamamoto, K. Tanaka, and T. Hirai. Wind Tunnel Installation Effects on Japan Aerospace Exploration Agency 's Standard Model. *Journal of Aircraft*, pages 1–22, 2022.